

Article

Experimental Study on Wave Current Characteristics and Stability of the Junction of Artificial Island and Subsea Tunnel

Longzai Ge, Hanbao Chen *, Songgui Chen and Haiyuan Liu

Tianjin Research Institute for Water Transport Engineering, National Engineering Research Center of Port Hydraulic Construction Technology, Tianjin 300456, China

* Correspondence: chenhanbao@tiwte.ac.cn

Abstract: In order to ensure the safety and reliability of the submerged tunnel covering layer at the junction of an artificial island and tunnel under extremely bad conditions, the wave current characteristics and the stability of the protective structure in the variable slope section were studied. By conducting model tests, the coupling effect of wave and current is revealed in this study. The hydrodynamic field, including the varying angles between waves and currents, is simulated in the model test. The ratio (H'_s/H_s) of the wave height and the ratio (U'/U) of the velocity with and without the existence of a current, the relative velocity (U/C), the wave steepness (H_s/L), the relative water depth (d/L) and the angle (α) between wave and current are obtained, and the corresponding calculation expression is derived, by checking the test results, the empirical formula can better predict the changes of wave height and water flow after wave current coupling. The stable weight of the surface protection rock is obtained through an optimization test. Based on the relationship between the stable weight of the protection rock and the wave height under the wave–current coupling effect, a modified expression for calculating the stable weight of the armor block is derived. The modified calculation method can support estimating the stable weight of the armor rocks of an overburden structure of a similar immersed tunnel under the wave–current coupling effect. This study can not only solve the practical problems of major projects of the Shenzhen–Zhongshan channel but also provide valuable basic data and technical support for the construction of overburden of subsea-immersed tube tunnels in the future.

Keywords: Shenzhen–Zhongshan channel project; overburden of immersed tube tunnel; wave–current coupling; stability; model test



Citation: Ge, L.; Chen, H.; Chen, S.; Liu, H. Experimental Study on Wave Current Characteristics and Stability of the Junction of Artificial Island and Subsea Tunnel. *J. Mar. Sci. Eng.* **2022**, *10*, 1525. <https://doi.org/10.3390/jmse10101525>

Academic Editor: Eva Loukogeorgaki

Received: 8 September 2022

Accepted: 14 October 2022

Published: 18 October 2022

Publisher's Note: MDPI stays neutral with regard to jurisdictional claims in published maps and institutional affiliations.



Copyright: © 2022 by the authors. Licensee MDPI, Basel, Switzerland. This article is an open access article distributed under the terms and conditions of the Creative Commons Attribution (CC BY) license (<https://creativecommons.org/licenses/by/4.0/>).

1. Introduction

According to incomplete statistics, more than 100 cross-sea and channel traffic tunnels have been built abroad in the past 100 years. These cross-sea traffic tunnel construction achievements [1–5] provide a good reference value for similar projects in China. At the same time, as a cross-sea passage, it has the characteristics of a high traffic rate and small impact on the environment, so its application prospect is wide.

In recent years, for long-distance cross-sea passage, a new combination mode of connecting with subsea tunnels through a new artificial island in open waters has been adopted. At the junction of the island and the tunnel, it is quite different from the connection between a traditional tunnel and the near-shore land and faces many new difficulties in design, mainly including: (1) the difficulty in obtaining the design wave elements is due to the artificial island's wave prevention requirements, the island's land elevation is higher than the extremely high water level, and the submarine tunnel needs to be connected with it by changing the slope. After the abrupt terrain is artificially constructed, it is easy to form the impact of wave breaking, current blocking, backwater and other local hydrodynamic environment deterioration; (2) the difficulty in determining the stable weight of overburden blocks is due to the construction of artificial islands in open waters and

the existence of headlands in the joint section, which has poor wave shielding and easily forms a concentration of wave energy. The common calculation formula of stable weight can no longer be applied; (3) it is difficult to determine the thickness of the overburden because the junction is located in the area of frequent water level changes, which is affected by the uncertainty of the degree of the wave–current coupling impact. (4) It is difficult to determine the interaction between the islands and tunnel; for the effect of the landscape, the western man-made island connected with an immersed tunnel is designed to be similar to the shape of traditional Chinese kites. Based on the previous research results [6], it is found that complex boundary conditions such as wave energy concentration and vortex negative pressure are generated at the corners and end of the island.

How to determine the stability of the overburden rock or block at the junction of the island and the tunnel under adverse influence conditions, such as steep gradient, complex hydrodynamic environment and the interaction between the island and the tunnel, is a very complex subject. At this time, the stability is not only affected by the coupling of simple waves and currents but also related to the structural cross-section type of the junction tunnel, artificial island and island. Referring to the previous studies on the stability of the junction between the island and the tunnel at home and abroad, very few similar results have been obtained, most of which tend to be in the anti-scour cover of flat deep-sea oil pipelines, as well as the stability of port breakwaters, bank revetments and bottom protection blocks or blocks.

Achievements in the overburden of deep seabed oil pipelines are as follows. Thusyathan [7] obtained the method for determining the stability of rock blocks by using the critical shear stress theory of rock block starting. Van gent and Wallast [8] carried out tests under the combined action of wave and current and derived the calculation formula of rock instability, which is also recommended by the CIRIA Rock Handbook [9].

$$\frac{S}{\sqrt{N}} = 0.2\theta^3 \quad (1)$$

$$\theta = \frac{u_0^2}{g\Delta D_{50}} \quad (2)$$

where N is the number of waves experienced in the whole design life of the rock pile; S is loss area of the rock cross section; θ is the judgment parameter of the rock block instability; u_0 is the maximum velocity of waves on the surface of the block; Δ is the ratio of stone density to seawater density.

Tørum et al. [10] took the block stone covering the submarine oil and gas pipeline as the object and obtained the critical value of the allowable instability rate. Wang [11] studied the stability of the riprap protective layer of the Hainan networking project and gave the stone grading; Wang et al. [12] took the riprap overburden of the Liwan 3-1 pipeline as an example, combined with the stability of stones, and calculated the grading method of stones that met the requirements; Wang et al. [13] conducted a physical model test on the treatment of pipe suspension by a local stone throwing method and obtained the stable particle size of stones at different flow rates; Xu et al. [14] determined the size of the riprap block through calculation analysis and experimental research in the submarine cable riprap protection project in Qiongzhou Strait. Sun [15] constructed a design method and calculation formula for stone particle size and recommended the characteristic particle size of stones for riprap calculation of a submarine pipeline in the South China Sea.

Achievements have been made in the stability of port breakwater and revetment toe protection. Some researchers, at home and abroad [16–27], have studied the stability of rock blocks at the toe protection of different structural sections of port breakwater under the action of different medium and long-term waves and currents, obtained the stable weight of blocks or stones and proposed the corresponding calculation formula for the stable weight according to the test results. In the design, the formula for calculating the stable weight of rock blocks or blocks at the toe of the slope is often given by using the

wave height and flow velocity in the Code for Design for Breakwater and Revetment [28] (JTS154-2018). See Equations (3)–(5) for details.

$$W = 0.1\gamma_b \left(\frac{\gamma}{\gamma_b - \gamma} \right)^3 \frac{H^2 L}{N_D^3} \quad (3)$$

$$N_D = 5.95 - 7.15 \ln \left(\frac{d + h_c}{d} \right) \quad (4)$$

$$U = \frac{\pi H}{\sqrt{\frac{\pi L}{g} \sinh \left(\frac{4\pi d}{L} \right)}} \quad (5)$$

where W is the stable weight of block; γ_b , γ is the gravity of rock block and water, respectively; H is the design wave height; N_D is the stability coefficient of the submerged embankment block; L is the wavelength; d is the water depth in front of the embankment; h_c is the height of the embankment top above the calculated water level. U is the maximum wave-generated bottom velocity in front of the embankment.

In addition, a few achievements have been made in the stability of submarine-immersed tube tunnels; most of them mainly involve the stability of the foundation of immersed tube tunnels under dynamic conditions such as waves and earthquakes. For example, Chen et al. [29–31] and Kasper et al. [32] proposed that the foundation of immersed tube tunnels will produce different response deformation under the action of waves, which will lead to foundation liquefaction or local erosion instability.

To sum up, since the previous research results rarely involve the stability of the blocks or stones of the overburden at the junction of the island and the tunnel, the design boundary conditions are difficult to obtain, and the local hydrodynamic conditions are complex, based on the above problems, a 1:40 model test study was carried out to ensure the structural safety of the Shenzhen–Zhongshan channel-immersed tube tunnel of the “century project”. This study can not only solve the practical problems in the project but also provide valuable test data and references for the future construction of island-immersed tube tunnels in China.

2. Physical Model Test

2.1. Engineering Background

The Shenzhen–Zhongshan channel is another supercluster project integrating “bridge, island, tunnel and underwater interchange” after Hong Kong Zhuhai Macao Bridge. It is located in the core area of Guangdong Hong Kong Macao Great Bay area and is constructed according to the standard of a two-way eight-lane expressway. The design speed of the tunnel is 100 km per hour. With a total length of 6.8 km, the subsea tunnel is the longest and widest subsea-immersed tube tunnel in the world, consisting of 32 pipe sections. The standard pipe section is 165 m long, 46 m wide and 10.6 m high. See Figure 1 [33] for the project layout. As the frequency of extreme bad weather has increased in recent years, the immersed tube tunnel is likely to encounter more severe natural environment tests than the initial design conditions in the design service period. In order to ensure the safety and reliability of the tunnel and improve the basic design data, physical model test research of the junction of the artificial island and tunnel is carried out.

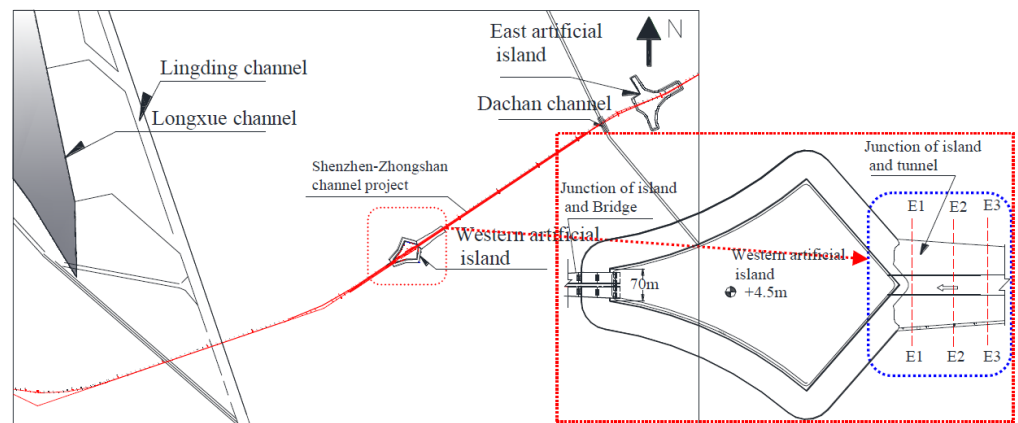


Figure 1. Layout plan of the project.

2.2. Test Design

2.2.1. Model Design and Creation

1. Structural case

The total length of the joint between the test simulation island and the tunnel is 400 m, including the covering layer of the E1–E3 pipe joint in the slope-changing section. The top elevation is from the joint of the west artificial island to the elevation of -8.3 m of the E3 pipe joint. Except for the 8000 kg Accropode block on both sides of the E1–E2 pipe joint in the area where the water level changes frequently, the other surfaces are protected with 1000~3000 kg block stones. The 100–200 kg block stones were used for the bottom protection, and the slope is 1:2.

See Figure 2 for the structural section of the covering layer at the joint.

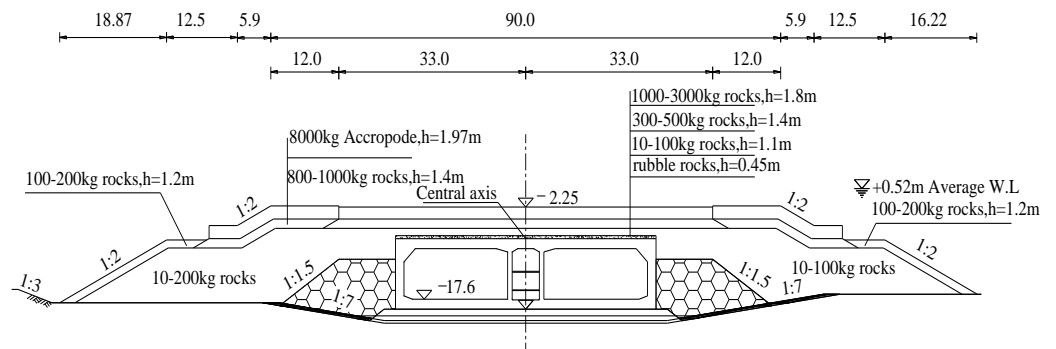


Figure 2. Section of overburden of immersed tunnel (unit: m).

2. Model design and production

According to the provisions of the Technical Code for Simulation Test of Water Transport Engineering (JTJ/T231-2021) [34], the normal model was adopted and designed according to the similarity law of the Froude number. The scale of each physical quantity simulated is as follows: geometric scale $L_r = 1:40$; time scale $T_r = L_r^{1/2}$; weight scale $M_r = L_r^3$; wave force scale $F_r = L_r^3$; pressure scale $P_r = L_r$; wave height scale $H_r = L_r$.

The test was carried out in a 40 m wide and 40 m long harbor basin, which is equipped with 40 light horizontal pusher wave making units, each with a width of 1.0 m. The maximum wave making capacity of the wave maker is: the water depth is 0.5 m, the wave height is 0~0.3 m, and the period is 0.5~3.0 s. At the same time, each unit can be freely spliced to achieve multi-directional wave making. In order to reduce wave boundary reflection, wave absorbers were set around the harbor basin.

The model test of the junction of the island and the tunnel includes two parts, namely, the 400 m long E1–E3 immersed tube tunnel and the 630 m long west artificial island. The

terrain within the simulation range was copied by the pile point method, with a height of 1.0×1.0 m, and the elevation was controlled by level; the shape of the west artificial island and immersed tube tunnel was controlled by erecting the broken plate, and the shape was reduced by a geometric scale of 1:40. All errors met the requirements of the test procedures. See Figure 3 for the model creation.

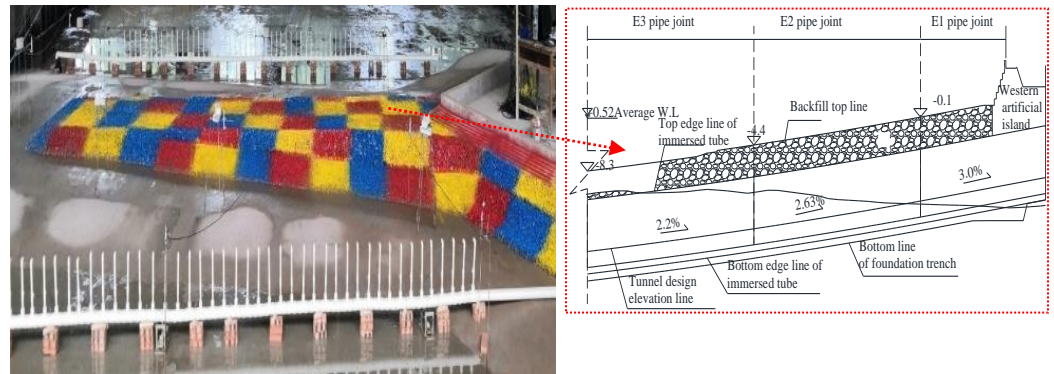


Figure 3. Completion of model making.

2.2.2. Working Condition Design and Boundary Simulation

1. Test condition design

Determination of water level: considering the influence of the stability of overburden blocks in the water level fluctuation area, four water levels, namely, 3.61, 1.89, 0.56 and -1.41 m, were selected according to the tidal level change in the project sea area. Wave determination: the wave element adopts the result corresponding to the water level. As for wave direction, the frequency of wave occurrence in the project sea area is high, and it has the most adverse impact on the stability of the overburden block or rock block at the junction. Therefore, three wave directions with angles of 45° , 90° and 135° with the axis from the island to the immersed tube tunnel were selected. Determination of water flow: according to the tidal current change in the project sea area, the most unfavorable to the stability, $U = 1.20$ m/s, was selected, and the constant flow mode was adopted. The water flow direction is in accordance with the rising and falling tide direction of the project sea area, i.e., the included angle with the axis from the island to the immersed tube tunnel is 45° , 90° , 135° , 225° , 270° and 315° . That is, the simulated water flow direction and the three wave directions are in the same direction and reverse direction, respectively. See Table 1 for the summary test conditions.

Table 1. Test conditions (note: the values in the table are prototype values).

Direction ($^\circ$)	Water Level (m)	Wave			Current	
		$H_{1\%}$ (m)	H_s (m)	T_p (s)	Direction/ $^\circ$	Velocity/(m/s)
45	3.61	4.15	2.88	7.90	$45^\circ / 225^\circ$	1.20
	1.89	3.80	2.64	7.57		
	0.56	3.72	2.60	7.44		
	-1.41	3.43	2.40	7.21		
90	3.61	4.12	2.87	7.89	$90^\circ / 270^\circ$	1.20
	1.89	4.06	2.83	7.84		
	0.56	3.97	2.77	7.66		
	-1.41	3.79	2.65	7.59		
135	3.61	3.96	2.75	8.88	$135^\circ / 315^\circ$	1.20
	1.89	3.84	2.67	8.75		
	0.56	3.62	2.53	8.26		
	-1.41	3.12	2.17	7.89		

2. Environmental simulation and methods

Wave simulation: irregular waves were used in the test, and according to the wave characteristics of the sea area of the project, the provisions on the wave spectrum in the Code of Hydrology for Harbor and Waterways (JTS145-2015) [35] were adopted. After the demonstration, the JONSWAP spectrum was determined to be the final spectrum ($\gamma = 3.3$). The number of irregular waves in each simulation was more than 120, and the simulation was repeated three times. The wave height and period error are controlled within $\pm 2\%$ of the specification. For the stability verification of blocks or stones, according to the requirements of the specifications, the duration of wave action shall not be less than 3 h.

Water flow simulation: 1#~6# reversible pumps are arranged on both sides of the harbor basin by using the intelligent control system of tidal current, and the different rotational speeds of the pumps were adjusted by controlling the frequency of each pump, so as to achieve the required water flow size and direction in the test basin.

Wave-current coupling simulation: before the test, the wave and current were calibrated, respectively, and the test wave height error was controlled within $\pm 2\%$ of the specification. During the test, the flow pattern required for the test was controlled in the harbor basin, and then the previously calibrated waves were superimposed and coupled under this state. Meanwhile, the TK2008 wave height collector and current meter independently developed by the company were used to monitor the wave height and flow velocity in the whole process.

2.2.3. Layout and Method of Measuring Points

The arrangement of wave height and water flow measurement points: within the simulation range of E1–E3 pipe joints, 9 measurement points were arranged along the tunnel axis at 3 sections. See Figure 4 for the arrangement of measurement points. The test data were monitored and analyzed by the TK2008 wave height acquisition system, and the test results were obtained.

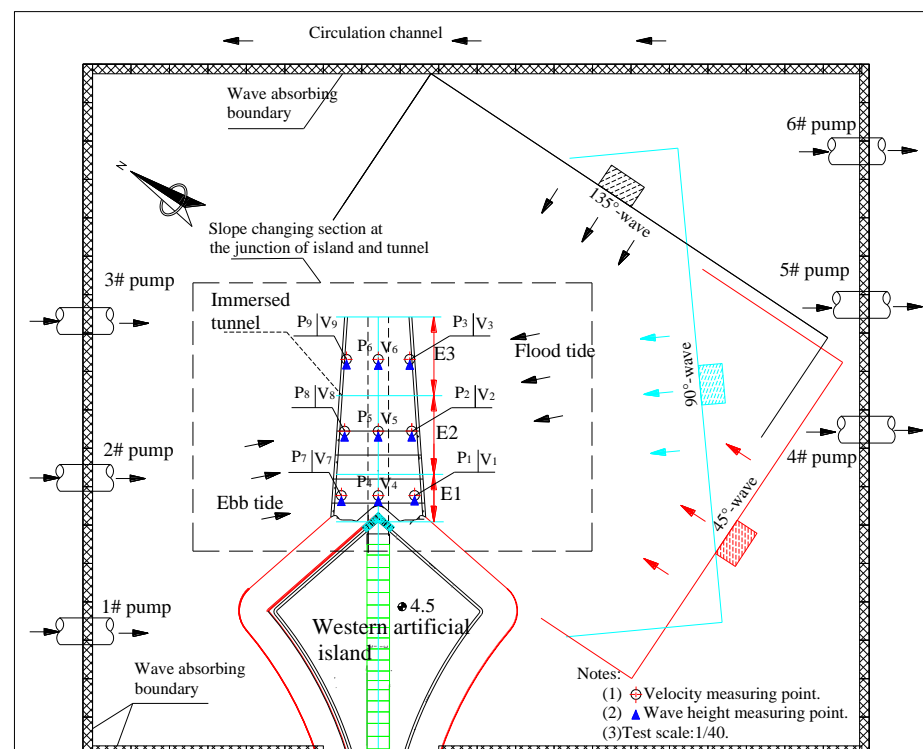


Figure 4. Layout of wave height and velocity measuring points.

Judgment method of block or rock stability: the judgment standard of block instability is that the block falls or the displacement accumulation exceeds half of the maximum

geometric scale of the block. The stability standard of rock blocks is that a small number of rock blocks are allowed to swing in situ under the action of waves, individual rock blocks are displaced, and the bottom protection surface is stable without obvious deformation. D (%) is used for the statistics of rock block instability. The calculation formula is shown in Formula (6). The statistical method is to count the number of rock block instabilities in each section and calculate the instability rate by comparing the photos taken before and after the test.

$$D = \frac{N_{dis}}{N_{total}} \times 100\% \tag{6}$$

where D is the total instability percentage; N_{dis} is the number of unstable rock blocks in each section; N_{total} is the total number of rock blocks in the corresponding section.

3. Results

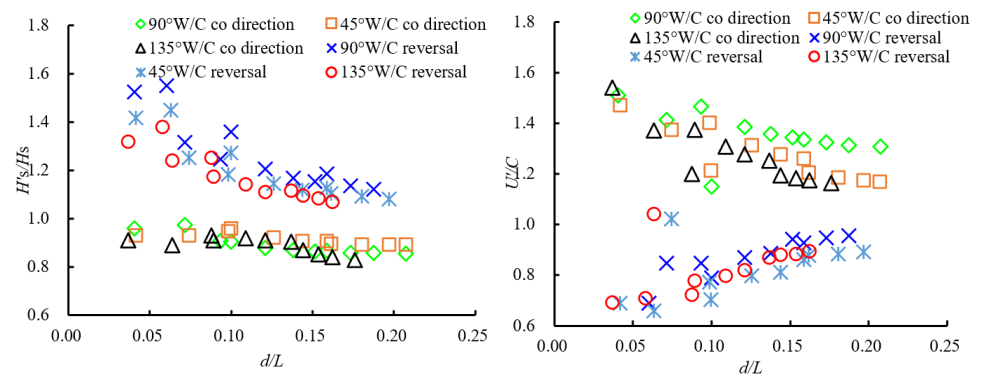
3.1. Wave Current Characteristics and Variation Law of Joint

For the junction of the island and the tunnel, it can be seen from the wave height and velocity results obtained from the test that the upstream side of the immersed tube tunnel is larger than the downstream side. See Table 2 for the wave height and velocity results of the measuring points on the upstream side under the most unfavorable working conditions of extreme high and low water levels. As can be seen from the table: (1) For wave height, the E3 position is smaller than the E1 position near the island, but affected by the steep gradient, the wave along the way is broken and the wave height decays quickly. For the flow rate, on the contrary, the E3 position is larger than the E1 position. (2) Influence of wave current angle: ① for a wave current in the same direction, compared with a single wave, affected by the flow velocity, the wave height decreases by 10~20%, but the wavelength increases by 15~25%. The effect on the water flow is the opposite. At this time, after the water flow superimposes the wave velocity, the water flow velocity increases as a whole, with an amplitude of 30~40% compared with the wave velocity. ② For the wave current reversal, compared with the single wave, the wave height increases by 20~45%, and the wavelength decreases by 10~20% due to the water jacking. When the wave velocity is superimposed on the corresponding water flow, the wave velocity decreases by 10~35%. ③ For the wave-current coupling, the wave velocity is still the main factor in the local velocity change. (3) Comparing the results of wave current angles of 45°, 90° and 135°, the amplitude of wave height change is 90° > 45° > 135°. The change in amplitude of flow velocity result is 90° > 135° > 45°.

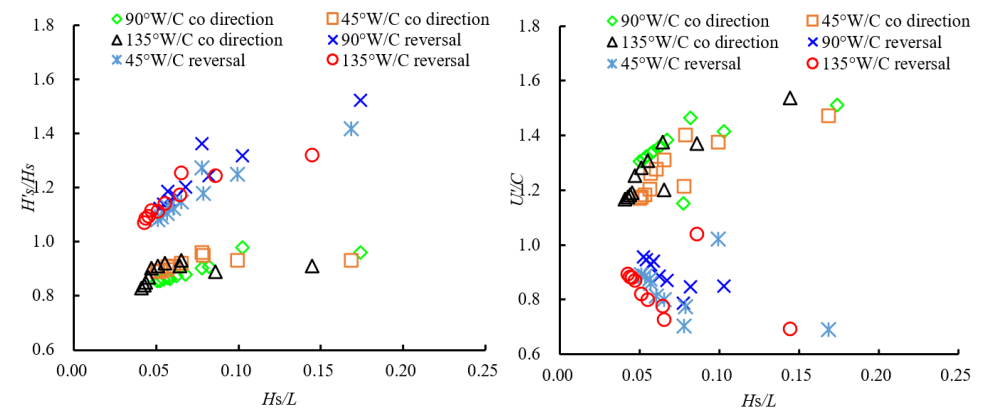
Table 2. Results of wave height and velocity at the junction under different wave-current couplings.

W.L (m)	Conditions	H_s (m)			Coupling Velocity of Wave and Current (m/s)		
		P1	P2	P3	V1	V2	V3
0.56	90° wave	2.72	2.47	2.62	2.67	3.78	6.18
	90° wave + 90° current	2.61	2.17	2.25	4.06	5.22	8.16
	90° wave + 270° current	4.21	3.06	3.01	1.23	3.21	5.81
3.61	90° wave	2.63	2.55	3.02	4.79	5.32	6.14
	90° wave + 90° current	2.36	2.19	2.59	5.51	7.07	8.04
	90° wave + 270° current	3.99	2.99	3.38	4.07	4.73	5.89
0.56	45° wave	2.50	2.34	3.01	2.66	3.76	6.12
	45° wave + 45° current	2.35	2.16	2.59	4.68	4.93	7.29
	45° wave + 225° current	3.3	2.77	3.31	1.33	2.9	5.45
3.61	45° wave	2.42	2.42	3.47	4.79	5.33	6.14
	45° wave + 45° current	2.32	2.21	2.84	5.8	6.71	7.18
	45° wave + 225° current	3.02	2.72	3.75	4.5	4.31	5.46
0.56	135° wave	1.87	2.02	1.6	2.05	5.58	5.74
	135° wave + 135° current	1.83	1.86	1.42	3.28	7.32	6.78
	135° wave + 315° current	2.97	2.36	1.76	0.78	4.36	5.05
3.61	135° wave	2.16	2.54	2.03	4.56	6.75	6.49
	135° wave + 135° current	2.05	2.28	1.81	5.47	8.43	7.6
	135° wave + 315° current	2.68	2.81	2.17	3.65	5.53	5.78

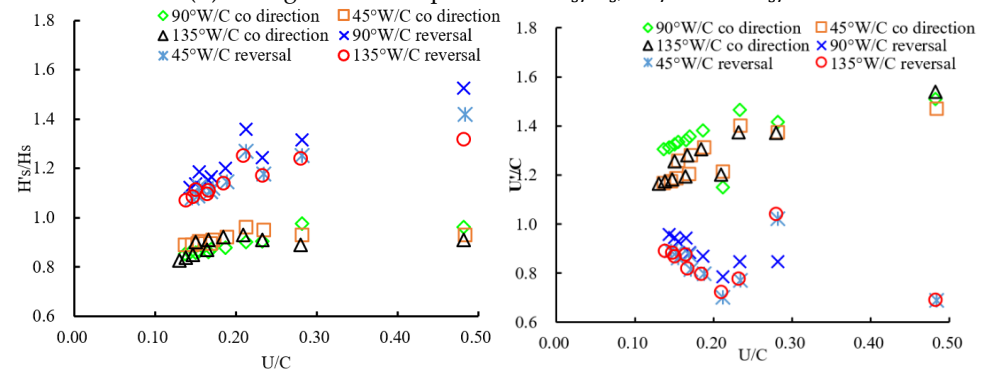
In order to further analyze the wave current characteristics of the steep slope section at the junction, the relationship between the wave height, velocity change rate ($H'_s/H_s, U'/C$) and $U/C, H_s/L, d/L$ under the wave–current coupling and single wave conditions is established, as shown in Figure 5. It can be obtained from the figure that: (1) for the wave current in the same direction, H'_s/H_s , the reverse U'/C value of wave and current, are all less than 1.0, with a change rate of 0.8~0.95. Comparing the effects of $U/C, H_s/L, d/L$ on wave height and velocity change rate, the sensitivity of d/L is stronger than that of U/C and H_s/L . According to the trend of wave height and velocity change rate, H'_s/H_s is positively proportional to U/C and H_s/L and inversely proportional to d/L . (2) For the wave current in reverse H'_s/H_s , the U'/C value of the wave and current in the same direction, with a change rate of 1.1–1.5, and the slope of change are significantly increased compared with that of waves in the same direction.



(a) Change relationship between $H'_s/H_s, U'/C$ and d/L



(b) Change relationship between $H'_s/H_s, U'/C$ and H_s/L



(c) Change relationship between $H'_s/H_s, U'/C$ and U/C

Figure 5. Change relationship between $H'_s/H_s, U'/C$ and $d/L, H_s/L, U/C$.

In order to further analyze the change rule of the wave spectrum after wave–current coupling at the junction of the island and tunnel, the wave measuring point in the middle of the combination of island and tunnel is selected, and the relationship between incident wave spectrum and wave current spectrum before and after wave–current coupling is given, as shown in Figure 6. As can be seen from Figure 6: (1) Compared with the three wave–current coupling angles, when the wave is 90° , the wave spectrum changes the most, and the minimum is a 45° wave; (2) compared with the incident wave, the wave spectrum energy increases to 1.7 times when the wave current is reversed and decreases to 0.8 times when the wave current is reversed.

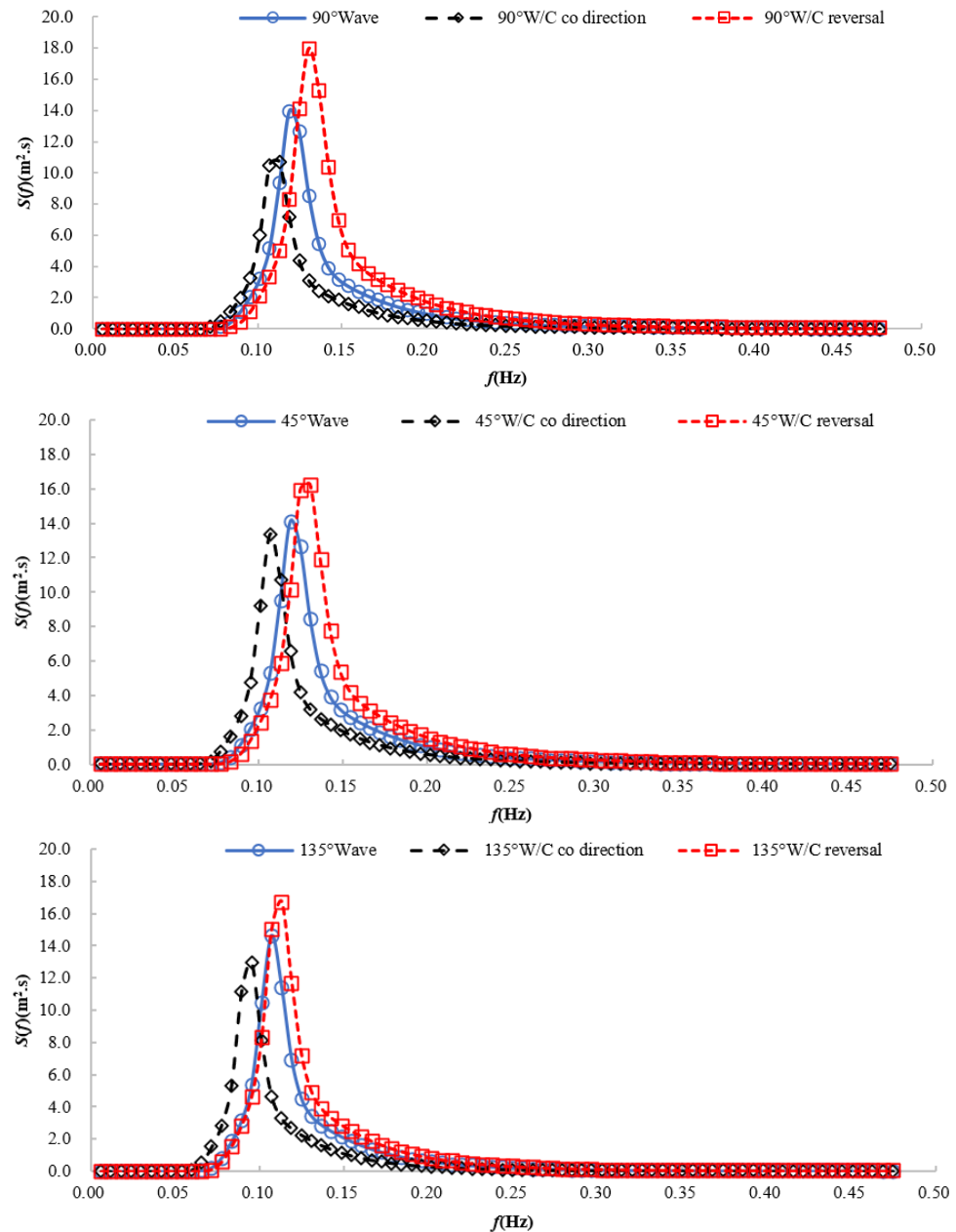


Figure 6. Comparison of wave spectrum before and after wave–current coupling at the junction of the island and tunnel.

3.2. Stability of Overburden Blocks or Stones

Based on the wave current characteristics of the above-mentioned junction, it can be seen that when the wave current has different included angles, the wave height and water flow increase significantly compared with the design. Meanwhile, complex wave conditions such as wave breaking and water level blocking occur in the variable slope section (see Figure 7a), which has a great impact on the stability of the overburden block or rock block. According to the experimental observation, the stability of the overburden in the E1 immersed tunnel with the most frequent water level fluctuation area is most affected. After the continuous wave action for 6 h, the instability numbers D (%) of the 1000~3000 kg protection block and 100~200 kg bottom protection block are 0.39% and 1.69%, respectively. According to the Code for Design of Breakwaters and Revetments (JTS154-2018) [28], the allowable instability rate is 1.0~2.0%. Therefore, it is considered that the block is stable. However, the first row of 8000 kg Accropode at the toe of the wave-facing side of the immersed tube tunnel loses the support of the seaside directional force and becomes unstable due to the wave suction generated by the wave trough (see Figure 7b). Through the optimization scheme of adding prism blocks weighing 800~1000 kg in front of the block, that is, increasing the support force of the outermost block and taking measures to shield and dissipate waves, the 8000 kg Accropode is stable under the wave–current coupling action, meeting the design requirements.



(a) Wave breaking along the overburden surface (b) Instability of 8 t Accropode at the toe of slope

Figure 7. Wave state and stability after wave–current coupling.

According to the stability of the overburden at the junction of the island and the tunnel, the area with the greatest impact on the stability after the wave–current coupling is: (1) the E1 pipe section area where the water level changes frequently at the junction; (2) block stones at the toe of the slope on the upstream side of the slope-changing section of the E1–E2 pipe joints; (3) the most unfavorable conditions leading to the block stability are 90° wave + 270° flow. The main reasons are analyzed as follows: (1) According to the test results in Table 3, under this condition, the wave height at the junction of the island and the tunnel changes the most. According to the block stability weight formula (3) in the paper, the block weight is in direct proportion to the square of the wave height, so the change in the wave height will quickly cause the weight change; (2) in addition, the block stability test results also show that the large wave height has the greatest impact on the block stability; (3) at the same time, according to the author's previous research results on block stability, wave height is one of the main factors causing block rock instability.

Table 3. Revision of design wave height cumulative frequency standard.

Type	Position	Design Content	Design Height F (%)	Revised Standard			
				Wave Current Reversal		Wave Current Co Direction	
				K_i	Height	K_i	Height
Vertical wall, pier	Superstructure, wall body, pier	strength, stability	$H_{1\%}$	1.2–1.6	1.2–1.6 $H_{1\%}$	0.75–0.95	$H_{5\%}$
	Subgrade bed, bottom protection rocks	stability	$H_{5\%}$		$H_{1\%}$		$H_{13\%}$
slop	Breast wall, embankment top block	strength, stability	$H_{1\%}$	1.2–1.6	1.2–1.6 $H_{1\%}$	0.75–0.95	$H_{5\%}$
	Armor blocks, rocks	stability	$H_{13\%}$ or $H_{5\%}$		$H_{5\%}$ or $H_{1\%}$		H or $H_{13\%}$
	Bottom protection rocks	stability	$H_{13\%}$		$H_{5\%}$		H

3.3. Calculation Method and Analysis of Stable Weight

1. Calculation method of wave height and velocity under wave–current coupling

Based on the above change rules, for the test results of H'_s/H_s , U'/C under wave–current coupling, in order to facilitate engineering calculation, empirical Formulas (7) and (8) between H'_s/H_s , U'/C and U/C , H_s/L , d/L , wave current angles are derived by referring to the test data. The calculation methods of H'_s/H_s , U'/C are as follows:

$$\frac{H'_s}{H_s} = 0.93 + 1.6 \sin(\alpha) \left[0.78 \left(\frac{H_s}{L} \right) - 0.19 \left(\frac{d}{L} \right) - 0.06 \left(\frac{H_s}{L} \right) \right] + 0.25\delta \sin(\alpha) \left(\frac{H_s}{d} \right) \quad (7)$$

$$\frac{U'}{U} = 0.95 + \sin(\alpha) \frac{C}{U} + 0.45\delta \left(\frac{H_s}{L} \right) = 1 + \frac{\sin(\alpha)}{U} \sqrt{\frac{2\pi g}{L} \tanh\left(\frac{2\pi d}{L}\right)} + 0.85\delta \left(\frac{H_s}{L} \right) \quad (8)$$

where α is the included angle between the wave, current and immersed tunnel axis ($^\circ$). δ is the wave current direction influence coefficient, take 1.0 for the same direction and -1.0 for the reverse direction. The meaning of other letters is the same as above.

In order to check the accuracy of the calculation Formulas (7) and (8), two sets of 90° and 180° test data are used to calculate H'_s/H_s and U'/U , and the test values and calculation results are shown in Figure 8. It can be seen from the figure that the data are basically located on both sides of the 45° slope line. In addition, the correlation analysis of the two sets of data shows that the correlation between H'_s/H_s and U'/U reaches more than 0.8 and 0.75, which indicates that the newly proposed empirical calculation Formulas (7) and (8) can better predict the changes in wave height and water flow after wave–current coupling.

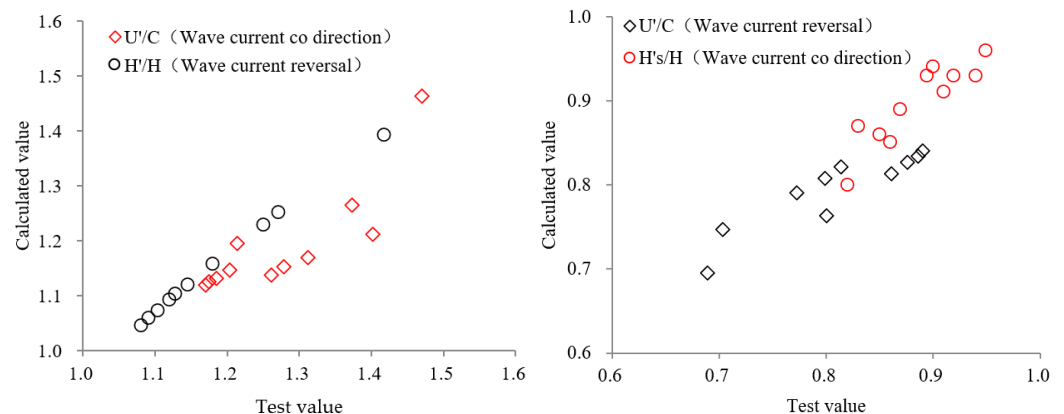


Figure 8. Verification results of test values and calculated values.

2. Revision of calculation method for the stable weight of block or rock

Referring to the calculation method of the stable weight of blocks or stones, it can be seen that the calculation formula mainly uses two expressions related to wave height or flow velocity. Therefore, for the revision of the calculation method, the change range of wave height or flow velocity is revised by introducing the influence coefficient K_i so as to achieve the goal of revising the calculation method.

① For the revision of the calculation method of the stable weight expressed by the wave height, that is, the revision of the design wave height standard, in combination with the requirements of the Code of hydrology for Harbor and Waterways (JTS145-2015) [35], and for the strength and stability calculation of hydraulic structures, the wave train accumulation frequency standard of the design wave height under normal conditions is determined according to the provisions in Table 3. However, after the wave–current coupling, the change rate of increase or decrease in wave height under different conditions is obtained. Therefore, the cumulative frequency standard of wave train of design wave height should be adjusted accordingly with the change in wave height, and the cumulative frequency standard of design wave height after adjustment can be finally obtained by using the conversion relationship (9) between the cumulative frequency and wave height. See Table 3.

$$H_F = \bar{H} \left[-\frac{4}{\pi} \left(1 + \frac{1}{\sqrt{2\pi}} H^* \right) \ln F \right]^{\frac{1-\bar{H}/d}{2}} \tag{9}$$

where H_F is the wave height with the cumulative frequency F ; \bar{H} is the average wave height.

Similarly, the current Formula (3) can also be revised by using the adjustment coefficient in Table 3. See Formula (10) for the revised calculation method.

$$W = 0.1\gamma_b \left(\frac{\gamma}{\gamma_b - \gamma} \right)^3 \frac{(H')^2 L_P}{N_D^3} = 0.1\gamma_b \left(\frac{\gamma}{\gamma_b - \gamma} \right)^3 \frac{(K_i H)^2 L_P}{N_D^3} \tag{10}$$

② for the revision of the calculation method of the stable weight expressed by the flow velocity, the research results are also used to achieve the revision goal of the calculation method by revising the design flow velocity value. Similarly, according to the requirements of the Code of Design for Breakwaters and Revetments (JTS154-2018) [28], the maximum wave bottom flow velocity in front of the breakwater toe is specified to determine the stable weight of the bottom protection block. The stable weight of the bottom protection block is determined according to Table 4. According to the test results of the flow velocity change after the wave–current coupling, adjust the stable weight of the bottom protection block, as shown in Table 4.

Table 4. Revision of stable weight of bottom protection block.

Design Value		Revised Value			
Maximum Wave Bottom Velocity (m/s)	Stable Weight of Rock (kg)	Wave Current Reversal		Wave Current Co Direction	
		K_i	Weight (kg)	K_i	Weight (kg)
2.0~2.5	60~100	1.15~1.45	100~200	0.70~0.90	Less than 60
2.6~3.0	100~200		200~300		60~100
3.1~3.5	200~300		300~400		100~200
3.6~4.0	300~400		400~600		200~300
4.1~4.5	400~600		600~800		300~400
4.6~5.0	600~800		Greater than 800		400~600

In addition, for the calculation method of the stable weight of blocks or stones, the adjustment coefficient K_i method is also used to revise the current calculation method. See Formula (11) for the revised calculation method.

$$W = \frac{\pi}{6} \gamma_s D_{50}^3 = \left[\frac{(K_i \times U)^2}{2gc^2 \frac{\gamma_s - \gamma}{\gamma}} \right]^3 \quad (11)$$

where c is the stability coefficient of rock block movement, taking 1.2 for the horizontal bottom slope and 0.9 for the inclined bottom slope.

4. Discussion

Based on the above experimental research results and considering the complexity of wave–current coupling, further research is needed in the future, mainly as follows: (1) only three representative wave directions with high frequency at the project location are selected in the paper, and the actual natural conditions have multi-directional effects on the wave current characteristics and stability, so the multi-directional wave–current coupling characteristics and stability research can be carried out for the island component junction in the next step. (2) The determination of the stable weight of the blocks or stones is also related to whether the waves are broken and the different positions of the structures. According to the requirements of the current specifications, the stable weight of the broken area still needs to be increased by no less than 25%; at the embankment head or the wave energy concentration position, the weight still needs to be increased by no less than 30%. Therefore, for the determination of the stable weight of blocks or stones, the designer needs to combine the actual situation of the project and comprehensively consider the influence of many factors to propose a reasonable stable weight. (3) When the derived empirical formulas H'_s/H_s and U'/U are applied, if there are prototype observation data, they can be further improved according to the actual results.

Through the test, it can be concluded that it is very necessary to use a physical model test for the stability study of the special area of the island component joint.

5. Conclusions

For the long-distance cross-sea passage, a new combination of an artificial island and subsea tunnel is adopted. Due to the few research results on wave current characteristics and overburden stability at the junction of an island and tunnel, and the difficulty in obtaining boundary conditions in design, a 1:40 model test is carried out to ensure the structural safety of the immersed tube tunnel of the Shenzhen–Zhongshan channel of the “century project”. The following results are obtained:

(1) Wave current characteristics and change rules at the junction of the island and the tunnel: ① for wave height, the E3 position is smaller than the E1 near the island, and the velocity is the opposite; ② the change values of H'_s/H_s in the same direction and U'/U in the opposite direction of the wave current are between 0.8 and 0.95, whereas the change values are between 1.1 and 1.5; ③ comparing the results of wave current angles of 45° , 90° and 135° , the variation amplitude of wave height is $90^\circ > 45^\circ > 135^\circ$. The change in amplitude of flow velocity result is $90^\circ > 135^\circ > 45^\circ$.

(2) Stability of overburden block: the instability number D (%) of the 1000~3000 kg block and 100–200 kg bottom protection block is 0.39% and 1.69%, respectively, meeting the requirements of the specification. However, 800 kg Accropode at the toe of the slope is unstable and stable after adopting the optimized scheme, which meets the design requirements. The most unfavorable conditions leading to the block stability are 90° wave + 270° flow.

(3) The wave height, flow velocity calculation method and stable weight are revised. ① Empirical formulas H'_s/H_s and U'/U are derived, which meet the accuracy requirements after verification by test results. ② The adjustment coefficient K_i after wave–current coupling is used to revise the existing formula, but in view of the complexity of wave–

current coupling, if there is prototype observation data during application, it can be further improved according to the actual results.

This study can not only solve the practical problems in the project but also provide valuable test data and technical references for the construction of immersed tube tunnels on islands in the future.

Author Contributions: L.G.: data collection, model design and testing, and data analysis; H.C.: data processing, comparison, and analysis; S.C.: model testing, data processing, comparison and analysis, and verification; H.L.: series group model testing, test instrument debugging, test terrain processing, and data verification. All authors have read and agreed to the published version of the manuscript.

Funding: This study was financially supported by the National Natural Science Foundation of China (52101316) special fund for central scientific research institutes (TKS20220301, TKS20210110) and Tianjin Science and Technology Foundation (Grant No. 21JCQNJC00480).

Institutional Review Board Statement: Not applicable.

Informed Consent Statement: Not applicable.

Data Availability Statement: Data sharing is applicable to this article, as new data were created or analyzed in this study.

Acknowledgments: This physical model test was conducted in the experimental harbor basin of the Tianjin Research Institute for Water Transport Engineering.

Conflicts of Interest: The authors declare no competing interests. The corresponding author is responsible for submitting a competing interest statement on behalf of all authors of the paper.

References

1. Dahlo, T.S.; Nilsen, B. Stability and rock cover of hard rock subsea tunnels. *Tunn. Undergr. Space Technol.* **1994**, *9*, 151–158. [[CrossRef](#)]
2. Vandebrouk, P. The channel tunnel: The dream becomes reality. *Tunn. Undergr. Space Technol.* **1995**, *10*, 17–21. [[CrossRef](#)]
3. Hagelia, E. Semi-quantitative estimation of water shielding requirements and optimization of rock cover for sub-sea road tunnels. *Int. J. Rock Mech. Min. Sci. Aeromechanics Abstr.* **1995**, *32*, 485–492.
4. Tsuji, H.; Sawada, T.; Takizawa, M. Extraordinary inundation accidents in the Seikan undersea tunnel. *Int. J. Rock Mech. Min. Sci. Aeromechanics Abstr.* **1996**, *119*, 1–14.
5. Palmstrom, A.; Skogheim, A. New Milestones in subsea blasting at water depth of 55 m. *Tunn. Undergr. Space Technol.* **2000**, *15*, 65–68. [[CrossRef](#)]
6. Ge, L.Z.; Cai, C.S.; Hu, P. Influence of the Shenzhen-Zhongshan channel west artificial island shape on stability of armor block and overtopping rate of crest. *Port. Waterw. Eng.* **2020**, *7*, 1–6. [[CrossRef](#)]
7. Thusyanthan, N.I.; Jegandan, S.; Robert, D.J. Stability of rock beam under wave and current loading. In Proceedings of the Twenty-Third (2013) International Offshore and Polar Engineering, Anchorage, AK, USA, 30 June–5 July 2013.
8. Van Gent, M.A.R.; Wallast, I. Stability of near-bed structures under waves and currents. In Proceedings of the 28th International Coastal Engineering Conference, Cardiff, Wales, 7–12 July 2002; World Scientific Publishing: Singapore, 2002.
9. CIRIA; Engineering CCFC; CETMEF. *The Rock Manual—The Use of Rock in Hydraulic Engineering C683*, 2nd ed.; CIRIA: London, UK, 2007.
10. Tørum, A.; Arntsenø, A.; Kuester, C. Stability against waves and currents of gravel rubble mounds over pipeline and flat gravel beds. In Proceedings of the 32th International Coastal Engineering Conference, Shanghai, China, 30 June–5 July 2010; World Scientific: Singapore, 2010; pp. 1–11.
11. Wang, Y.S. Follow-up Engineering Construction of Riprap Protection for 500 kV Submarine Cable. *Electr. Power Constr.* **2012**, *33*, 116–118. [[CrossRef](#)]
12. Wang, M.; Sun, G.M. Application of fall-pipe rock placement technology in Liwan3-1 export offshore pipeline. *Ocean. Eng.* **2015**, *3*, 90–96. [[CrossRef](#)]
13. Wang, Y.; Li, J.; Sun, C.B. Experiment study on the local rock dumping methods for submarine pipeline spans. *Oil Gas Storage Transp.* **2016**, *7*, 784–787. [[CrossRef](#)]
14. Xu, G.; Ji, J.N.; Qu, H.L. Calculation and experimental research on stable dimension of rockfill. *Shandong Sci.* **2018**, *31*, 127–132. [[CrossRef](#)]
15. Sun Qing. Riprap stone size design of protective structure for deepwater submarine pipeline. *Pet. Eng. Constr.* **2021**, *47*, 18–22. [[CrossRef](#)]
16. Zhong, J.; Tang, Z.Y.; Shen, Y.S. Stability of the toe rocks of the rubble-mound breakwater under swell action. *Port. Waterw. Eng.* **2020**, *64*–71. [[CrossRef](#)]

17. Clemente, D.; Calheiros-Cabral, T.; Rosa-Santos, P.; Taveira-Pinto, F. Hydraulic and Structural Assessment of a Rubble-Mound Breakwater with a Hybrid Wave Energy Converter. *J. Mar. Sci. Eng.* **2021**, *9*, 922. [[CrossRef](#)]
18. Ma, B.; Liang, S.; Liang, C.; Li, Y. Experimental Research on an Improved Slope Protection Structure in the Plunge Pool of a High Dam. *Water* **2017**, *9*, 671. [[CrossRef](#)]
19. Gerding, E. Toe structure stability of rubble mound breakwaters. In *Delft and Delft Hydraulics Report H1874*; Delft University of Technology: Delft, the Netherlands, 1993.
20. USACE. Coastal Engineering Manual Part VI: Design of Coastal Project Elements. In *Place of Publication Not Identified*; Books Express Publishing: Berkshire, UK, 2012.
21. Van Gent, M.R.A. Rock stability of rubble mound breakwaters with a berm. *Coast. Eng.* **2013**, *78*, 35–45. [[CrossRef](#)]
22. Van Gent, M.R.A.; van der Werf, I.M. Rock toe stability of rubble mound breakwaters. *Coast. Eng.* **2014**, *83*, 166–176. [[CrossRef](#)]
23. Etemad-Shahidi, A.; Bali, M. Stability of rubble-mound breakwater using H50 wave height parameter. *Coast. Eng.* **2012**, *59*, 38–45. [[CrossRef](#)]
24. Van der Meer, J.W. Stability of breakwater armor layers—Designs formulae. *Coast. Eng.* **1987**, *11*, 219–239. [[CrossRef](#)]
25. Hudson, R.Y. *Design of Quarry Stone Cover Layer for Rubble Mound Breakwaters*; Waterways Experiment Station, Coastal Engineering Research Centre: Vicksburg, MS, USA, 1958.
26. Vidal, C.; Medina, R.; Lomónaco, P. Wave height parameter for damage description of rubble-mound breakwaters. *Coast. Eng.* **2006**, *53*, 711–722. [[CrossRef](#)]
27. Chen, W.; Wang, D.; Xu, L.; Lv, Z.; Wang, Z.; Gao, H. On the Slope Stability of the Submerged Trench of the Immersed Tunnel Subjected to Solitary Wave. *J. Mar. Sci. Eng.* **2021**, *9*, 526. [[CrossRef](#)]
28. Ministry of Transport. *Code of Design for Breakwaters and Revetments*; People's Communications Publishing House Co., Ltd.: Beijing, China, 2018.
29. Chen, W.Y.; Fang, D.; Chen, G.X.; Jeng, D.S.; Zhu, J.F.; Zhao, H.Y. A simplified quasi-static analysis of wave-induced residual liquefaction of seabed around an immersed tunnel. *Ocean Eng.* **2018**, *148*, 574–587. [[CrossRef](#)]
30. Chen, G.X.; Ruan, B.; Zhao, K.; Chen, W.Y.; Zhuang, H.Y.; Du, X.L.; Khoshnevisan, S.; Juang, C.H. Nonlinear Response Characteristics of Undersea Shield Tunnel Subjected to Strong Earthquake Motions. *J. Earthq. Eng.* **2020**, *24*, 351–380. [[CrossRef](#)]
31. Chen, W.Y.; Liu, C.L.; Duan, L.L.; Qiu, H.M.; Wang, Z.H. 2D Numerical Study of the Stability of Trench under Wave Action in the Immersing Process of Tunnel Element. *J. Mar. Sci. Eng.* **2019**, *7*, 57. [[CrossRef](#)]
32. Kasper, T.; Steinfeldt, J.S.; Pedersen, L.M.; Jackson, P.G.; Heijmans, R.W.M.G. Stability of an immersed tunnel in offshore conditions under deep water wave impact. *Coast. Eng.* **2008**, *55*, 753–760. [[CrossRef](#)]
33. Yao, Z.A.; Chen, B.Y. Key Construction Techniques for Foundation Pit Supporting Structure of East Anchor Block of Lingdingyang Bridge. *Bridge Constr.* **2020**, *50*, 105–110. [[CrossRef](#)]
34. Ministry of Transport. *Technical Code for Simulation Test of Water Transportation Engineering*; People's Communications Publishing House Co., Ltd.: Beijing, China, 2021.
35. Ministry of Transport. *Code of Hydrology for Harbor and Waterway*; People's Communications Publishing House Co., Ltd.: Beijing, China, 2015.